# Photoelectric disintegration of $^{16}$O

M. Katsuma*
*Advanced Mathematical Institute, Osaka City University, Osaka 558-8585, Japan*

(Received 4 September 2014; revised manuscript received 10 November 2014; published 5 December 2014)

The photoelectric cross section of $^{16}$O$(\gamma,\alpha)^{12}$C is estimated to be larger than the radiative capture cross section of $^{12}$C$(\alpha,\gamma)^{16}$O. The predicted cross section and the angular distribution of the $\alpha$ particle are illustrated for the future experiment. The cross section just above the $\alpha$-particle threshold is found to be dominated by the $E2$ excitation.

DOI: 10.1103/PhysRevC.90.068801 PACS number(s): 25.20.−x, 25.40.Lw, 26.20.Fj, 24.50.+g

The low-energy $^{12}$C$(\alpha,\gamma)^{16}$O reaction plays a crucial role in the nucleosynthesis of elements in a star. However, the cross section is very small at energies corresponding to helium burning temperatures, $E_{\rm c.m.} \approx 0.3$ MeV, because of the Coulomb barrier, and it is far out of reach by present laboratory technologies [1]. ($E_{\rm c.m.}$ is the center-of-mass energy of the $\alpha + {}^{12}$C system.) To cope with these difficulties, experimental efforts have been made (e.g., [2–9]), as well as theoretical predictions [10,11]. Current experimental projects with high intensity lasers [2,12,13] are also trying to precisely measure the tiny cross section.

The probability of the photodisintegration of $^{16}$O just above the $\alpha$-particle threshold restricts the reaction rates of the $^{12}$C$(\alpha,\gamma)^{16}$O reaction. In particular, the angular distribution of the emitted $\alpha$ particle is expected to reduce the large uncertainties of the cross section. The subthreshold $1_1^-$ state at the excitation energy $E_x = 7.12$ MeV has been believed to couple strongly with the $1_2^-$ state at $E_x = 9.585$ MeV. The strong interference in two $1^-$ states leads to the large enhancement of the low-energy cross section, and it has been presumed to play an important role in the derived reaction rates at helium burning temperatures. In contrast, Refs. [10,11,14] have predicted that the $E1$ cross section is not enhanced by the high energy tail of the subthreshold $1_1^-$ state because the $\alpha + {}^{12}$C system can be described by the weak coupling. In addition, the low-energy cross section has been reported to be dominated by the $E2$ transition. This is endorsed by the $\gamma$-ray angular distribution at $E_{\rm c.m.} = 1.254$–$1.34$ MeV [8,9] and the transparency of the $\alpha + {}^{12}$C system at low energies [11,14–16].

In the present Brief Report, the photoelectric disintegration of $^{16}$O is studied with a potential model. The expected photoelectric cross section of the $^{16}$O$(\gamma,\alpha)^{12}$C reaction is illustrated with the reciprocity theorem. The purpose of this report is to show the prediction of the photoelectric cross section from the potential model [10].

The cross section of the $^{16}$O$(\gamma,\alpha)^{12}$C reaction is given by the inverse reaction in the following expression:

$$\sigma_{\gamma\alpha}(E_\gamma) = \frac{k_c^2}{2k_\gamma^2}\sigma_{\alpha\gamma}(E_{\rm c.m.}), \qquad (1)$$

where $k_c$ is the wave number of the relative motion between the $\alpha$ particle and the $^{12}$C nuclei; $k_\gamma$ is the wave number of the photon $k_\gamma = E_\gamma/(\hbar c)$, $E_\gamma = E_{\rm c.m.} + 7.162$ MeV; $\sigma_{\alpha\gamma}$ is the capture cross section for the $^{12}$C$(\alpha,\gamma)^{16}$O reaction. To obtain the predicted values, the same potential model as in [10] is adopted. The $\alpha$ particle does not emerge easily because of the Coulomb barrier in the $\alpha + {}^{12}$C channel. Consequently, $\sigma_{\gamma\alpha}$ is very small. To compensate for the rapid energy variation below the barrier, it is multiplied by the Gamow factor, $\exp(2\pi\eta)$, in the present report. $\eta$ is the Sommerfeld parameter, $\eta = Z_1 Z_2 e^2/(\hbar v)$. $Z_1$ and $Z_2$ are the charges of the interacting nuclei. $v$ is the velocity of relative motion between the $\alpha$ particle and $^{12}$C nuclei. The calculation displayed here is the cross section obtained with the unpolarized $\gamma$ ray, because the $^{12}$C$(\alpha,\gamma)^{16}$O cross section is made by the incoherent sum over two independent polarizations of the $\gamma$ ray [10,17].

The cross section of the photodisintegration is expected to be larger than that of the $^{12}$C$(\alpha,\gamma)^{16}$O reaction. From Eq. (1), $\sigma_{\gamma\alpha} \approx 50 \times \sigma_{\alpha\gamma}$ is found at $E_\gamma \approx 8.41$ MeV, corresponding to $E_{\rm c.m.} = 1.25$ MeV close to the lowest energy of the angular distribution measurement of $^{12}$C$(\alpha,\gamma)^{16}$O [9]. This means that the study of $^{16}$O$(\gamma,\alpha)^{12}$C gives the capture cross section and the $E2/E1$ ratio more accurately.

The calculated photoelectric cross section of the $^{16}$O$(\gamma,\alpha)^{12}$C reaction is shown in Fig. 1. The solid curve is the result obtained from the potential model. The dashed and dotted curves are the $E1$ and $E2$ components, respectively. The vertical thin line at $E_\gamma = 7.162$ MeV indicates the energy position of the $\alpha$-particle threshold in $^{16}$O. The $\alpha$ particle is emitted above this energy. The peak at the $1_2^-$ state can be seen at $E_\gamma \approx 9.5$ MeV. The $E1$ component is approximately constant below $E_\gamma = 8$ MeV. The photoelectric disintegration is found to be dominated by the $E2$ excitation below $E_\gamma \approx 8$ MeV. This is due to the high energy tail of the subthreshold $2_1^+$ state at $E_x = 6.92$ MeV, which has the well-developed $\alpha + {}^{12}$C cluster structure [14]. The photonuclear reaction may remind you of the discussion about the dipole excitation. However, the photomagnetic dipole excitation ($s$ wave) is forbidden. The electric dipole transition ($p$ wave) is hindered by the isospin selection rule. Thus, the $E2$ excitation ($d$ wave) could be the dominant mode of the transition in the vicinity of the $\alpha$-particle threshold. The $E3$ and $E4$ transitions ($f$ and $g$ waves) are negligible.

The $\sigma_{\gamma\alpha}\exp(2\pi\eta)$ in Fig. 1 resembles the astrophysical $S$ factor in the $^{12}$C$(\alpha,\gamma)^{16}$O reaction [10]. The energy variation, in fact, corresponds to $\sigma_{\gamma\alpha}\exp(2\pi\eta) \propto S/E_\gamma^2$.

*mkatsuma@sci.osaka-cu.ac.jp

 

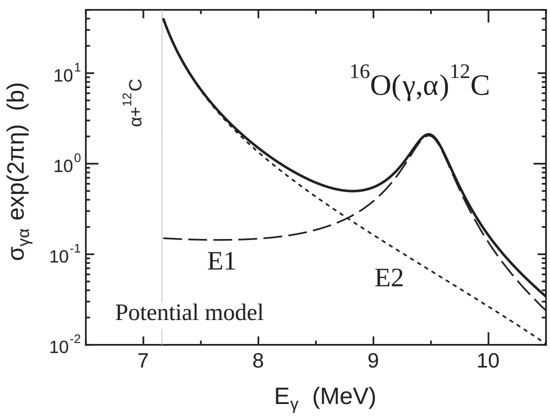


FIG. 1. Photoelectric cross section for the $^{16}$O($\gamma,\alpha$)$^{12}$C reaction as a function of the $\gamma$-ray energy. The solid curve is the result obtained from the potential model. The dashed and dotted curves are the $E1$ and $E2$ components, respectively. The cross section is multiplied by $\exp(2\pi\eta)$ to compensate for the rapid energy variation in the vicinity of the $\alpha$-particle threshold. The vertical thin line at $E_\gamma = 7.162$ MeV indicates the energy position of the threshold.

The angular distributions of the $\alpha$ particle at $E_\gamma = 8.0$, 8.5, 9.0, and 9.5 MeV are shown in Fig. 2. The solid curves are the results obtained from the potential model. $\theta$ is the angle between $\boldsymbol{k}_c$ and $\boldsymbol{k}_\gamma$. At $E_\gamma = 9.5$ MeV, the angular distribution appears to be the single peak due to the $1_2^-$ state at $E_x = 9.585$ MeV. The angular distribution becomes the double peaks at $E_\gamma = 8.0$ MeV. The dashed and dotted curves are the pure $E1$ and $E2$ components. The $E2$ contribution caused by the subthreshold $2_1^+$ state interferes in the dipole component.

The differential cross section at $\theta = 90^\circ$ is made only from the $E1$ component, because the $E2$ component vanishes at this angle. Using the 90° cross section, the integrated $E1$ cross section is expressed as

$$\sigma_{\gamma\alpha}^{E1}(E_\gamma) = \frac{8\pi}{3}\frac{d\sigma_{\gamma\alpha}}{d\Omega}\bigg|_{\theta=90^\circ}. \quad (2)$$

The dashed curve in Fig. 1 can be confirmed from this relation. The numerical values are listed in Table I.

The 90° cross section basically determines the $E1$ contribution of the photodisintegration of $^{16}$O. As shown in Fig. 2, the angular distribution has the minimum at $\theta \approx 90^\circ$ at low energies, because the $E2$ contribution becomes large. In addition, the total cross section is very small below the barrier. In this circumstance, the $E1$ component may be susceptible to the background noise. The absolute value of the $E1$ cross section could not be determined without precise measurement of the angular distribution. Hopefully, the $E2/E1$ ratio will be provided more accurately by the future experiment.

The calculated $\sigma_{E2}/\sigma_{E1}$ value is shown in Fig. 3. The solid curve is the result obtained from the potential model. As a comparison, the calculated value of [13] is also shown by the dot-dashed curve. The difference between the two curves at low energies stems from the assumed reaction mechanism. Reference [13] uses the compound nuclear model with the strong coupling. The potential model describes the direct reaction process, in which only a few degrees of freedom of motion are activated.

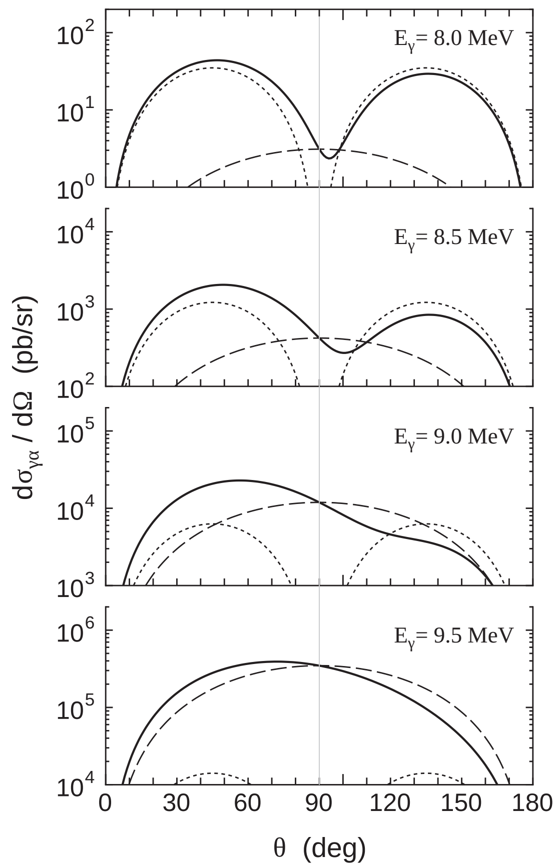


FIG. 2. Differential cross sections for the $^{16}$O($\gamma,\alpha$)$^{12}$C reaction at $E_\gamma = 8.0$, 8.5, 9.0, and 9.5 MeV. The solid curves are the results obtained from the potential model. The dashed and dotted curves are the pure $E1$ and $E2$ components.

Finally, let me describe a supplementary explanation about the angular distribution with a linearly polarized $\gamma$ ray. The angular distribution of $^{16}$O($\vec{\gamma},\alpha$) $^{12}$C is given from [17,18] as follows:

$$\frac{d\sigma_{\vec{\gamma}\alpha}}{d\Omega}(\theta,\phi) = \frac{d\sigma_{\gamma\alpha}}{d\Omega}(\theta)[\,1 + f\cos(2\phi)], \quad (3)$$

where $d\sigma_{\gamma\alpha}/d\Omega$ is the angular distribution by the unpolarized $\gamma$ ray shown in Fig. 2; $f$ is the linear polarization of the $\gamma$-ray beam, $f \approx 1$; the $\phi$ is the angle between the direction of polarization and the $x$ axis. The Cartesian coordinate is defined by the right-handed system: the $z$ axis is along with $\boldsymbol{k}_\gamma$; the $y$ axis is along with the vector $\boldsymbol{k}_\gamma \times \boldsymbol{k}_c$. The reaction occurs on the $x - z$ plane. The angular distribution varies with a factor of 0–2 by the direction of the polarization of $\gamma$-ray

TABLE I. Photoelectric dipole cross section and 90° cross section. The value of $\exp(2\pi\eta)$ is also listed.

| $E_\gamma$ (MeV) | $d\sigma_{\gamma\alpha}/d\Omega\,(90^\circ)$ (b/sr) | $\sigma_{\gamma\alpha}^{E1}$ (b) | $\exp(2\pi\eta)$ |
|---|---|---|---|
| 8.0 | $3.11 \times 10^{-12}$ | $2.60 \times 10^{-11}$ | $5.72 \times 10^9$ |
| 8.5 | $4.22 \times 10^{-10}$ | $3.53 \times 10^{-9}$ | $5.27 \times 10^7$ |
| 9.0 | $1.19 \times 10^{-8}$ | $9.98 \times 10^{-8}$ | $3.88 \times 10^6$ |
| 9.5 | $3.47 \times 10^{-7}$ | $2.91 \times 10^{-6}$ | $6.94 \times 10^5$ |

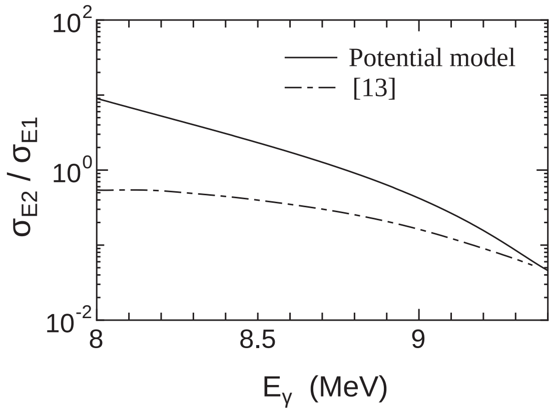


FIG. 3. Ratio of $E2$ component to $E1$ in $^{16}O(\gamma,\alpha)^{12}C$. The solid curve is the result obtained from the potential model. The dot-dashed curve is from the resonance theory [13], of which the value is taken from Fig. 2 of [13].

beam [13]. From Eq. (3), the $d\sigma_{\gamma\alpha}/d\Omega$ of Fig. 2 is found to give the basic quantities of the photoelectric disintegration of $^{16}O$, even when a linearly polarized $\gamma$ ray is used.

In summary, the $^{16}O(\gamma,\alpha)^{12}C$ reaction has been studied with the potential model. The calculated photoelectric cross section and the angular distribution of the $\alpha$ particle have been shown in figures. The cross section just above the $\alpha$-particle threshold is dominated by the $E2$ excitation. The cross section of the photoelectric disintegration is found to be larger than that of the $^{12}C(\alpha,\gamma)^{16}O$ reaction. Therefore, the forthcoming experimental projects [2,12,13] are expected to determine the $^{12}C(\alpha,\gamma)^{16}O$ cross section more accurately.

I am grateful to Prof. Moshe Gai and Prof. M. Fujiwara for their encouragement. I thank Y. Kondō for early days of collaboration and Y. Ohnita and Y. Sakuragi for their hospitality. I also thank M. Arnould, A. Jorissen, K. Takahashi, and H. Utsunomiya for their hospitality during my stay at the Université Libre de Bruxelles.

[1] C. E. Rolfs and W. S. Rodney, *Cauldrons in the Cosmos* (University of Chicago, Chicago, 1988).
[2] M. Gai, Nucl. Phys. A **928**, 313 (2014).
[3] M. Gai, Phys. Rev. C **88**, 062801 (2013).
[4] C. R. Brune and D. B. Sayre, J. Phys.: Conf. Ser. **420**, 012140 (2013).
[5] D. Schürmann, L. Gialanella, R. Kunz, and F. Strieder, Phys. Lett. B **711**, 35 (2012).
[6] R. Plag, R. Reifarth, M. Heil, F. Käppeler, G. Rupp, F. Voss, and K. Wisshak, Phys. Rev. C **86**, 015805 (2012).
[7] H. Makii, Y. Nagai, T. Shima, M. Segawa, K. Mishima, H. Ueda, M. Igashira, and T. Ohsaki, Phys. Rev. C **80**, 065802 (2009).
[8] M. Assunção, M. Fey, A. Lefebvre-Schuhl, J. Kiener, V. Tatischeff, J. W. Hammer, C. Beck, C. Boukari-Pelissie, A. Coc, J. J. Correia *et al.*, Phys. Rev. C **73**, 055801 (2006).
[9] R. Kunz, M. Jaeger, A. Mayer, J. W. Hammer, G. Staudt, S. Harissopulos, and T. Paradellis, Phys. Rev. Lett. **86**, 3244 (2001).
[10] M. Katsuma, Phys. Rev. C **78**, 034606 (2008); **81**, 029804 (2010); Astrophys. J. **745**, 192 (2012).
[11] M. Katsuma, arXiv:1404.3966.
[12] M. Ahmed, A. Champagne, B. Holstein, C. Howell, W. Snow, R. Springer, and Y. Wu, arXiv:1307.8178.
[13] Y. Xu, W. Xu, Y. G. Ma, W. Guo, J. G. Chen, X. Z. Cai, H. W. Wang, C. B. Wang, G. C. Lu, and W. Q. Shen, Nucl. Instrum. Methods A **581**, 866 (2007).
[14] M. Katsuma, Phys. Rev. C **81**, 067603 (2010); J. Phys. G **40**, 025107 (2013); EPJ Web Conf. **66**, 03041 (2014).
[15] P. Tischhauser, A. Couture, R. Detwiler, J. Görres, C. Ugalde, E. Stech, M. Wiescher, M. Heil, F. Käppeler, R. E. Azuma *et al.*, Phys. Rev. C **79**, 055803 (2009).
[16] R. Plaga, H. W. Becker, A. Redder, C. Rolfs, H. P. Trautvetter, and K. Langanke, Nucl. Phys. A **465**, 291 (1987).
[17] H. J. Rose and D. M. Brink, Rev. Mod. Phys. **39**, 306 (1967).
[18] H. R. Weller, J. Langenbrunner, R. M. Chasteler, E. L. Tomusiak, J. Asai, R. G. Seyler, and D. R. Lehman, At. Data Nucl. Data Tables **50**, 29 (1992).